Plasma Characteristics in the Discharge Region of a 20A Emission Current Hollow Cathode

Sun Ming-ming*[1], Song Jia-yao[2], GUO Wei-long[1], Wen Xiao-dong[1],
(1. Science and Technology on Vacuum Technology and Physics Laboratory，
Lanzhou Institute of Physics, Lanzhou 730000, China,
2.Weather Modification Office of Shaanxi Province, Xi'an 710014, China)

Abstract: In order to obtain the plasma characteristics in discharge region of LIPS-300 ion thruster's 20A emission current hollow cathode and verify the structure design of the emitter, numerical calculation method and finite element method were used to study plasma characteristics in the hollow cathode. The results of these methods indicate that the highest plasma density and electron temperature which improving significantly in orifice region is located in the discharge region of the hollow cathode. The magnitude of plasma density is about $10^{21}m^{-3}$ both in emitter region and orifice region, while decreases exponentially in plume region with the distance from the orifice exit. Meanwhile, compared to the orifice region, the electron temperature and current improved about 1~2eV and 36% in the emitter region respectively. The hollow cathode performance test results are in well agreement with numerical calculations, which proved that the structure design of emitter and orifice meets the requirements of 20A emission current. Although there are few mistakes occurred in finite element method, it still, however, can be used to estimate plasma characteristics at the beginning of hollow cathode design process due to its simplicity.

Key words: ion thruster； hollow cathode; plasma characteristics

I. Introduction

LIPS-300 is a high power, high thrust ion thruster which was designed for the new generation large-scale truss-type satellite platform in China[1]. In order to meet the technical requirements of LISP-300 ion thruster, a hollow cathode with a nominal emission current of 20A has been designed and manufactured as the primary electron source. As the processes of plasma discharge, generation and extraction have significant influences the emission current, it is woth studying the plasma characteristics in the hollow cathode which, besides, can also be used to verify the structure design of its emitter and orifice.

The hollow cathode discharge area can be divided into three regions: emitter region, orifice region and plume region, in which the discharge characteristics are distinctly different. The discharge characteristics of NEXIS ion thruster’s hollow cathode whose discharge current is 25A has been studied by Goebel et al.[2] which indicated that the magnitudes of plasma density are 10^{21} m^{-3} and 10^{23} m^{-3} in the emitter and orifice region respectively. After the plasma entering the plume region, the plasma density decreases rapidly to 1×10^{18} m^{-3} along with the increasing distance from the exit of orifice. Meanwhile, the electron temperature was found to be increased from the range of 1eV~2eV to the range of 2eV~3eV. In NSTAR ion thruster, calculated statistically by Katz et al.[3], almost one third of the total number of electrons emitted by TH15 hollow cathode is generated in orifice region and the plasma density would decrease one order if the orifice’s diameter increasing from 1mm to 2mm. The discharge characteristics study of 25A emission current hollow cathode in NEXIS ion thruster showed the similar results with in NSTAR ion thruster. The plasma potentials

in the emitter and orifice is in the range of 5~14V and 15~30V respectively. Meanwhile, the electron current density is in the range of 1×10^4~10^5 A/m^2 in the emitter region and increased more than 50% in the orifice region. These previous results were verified experimentally by Malik et al.[4], which also verified the reasonability of the emitter and orifice structure design of the hollow cathodes in NSTAR and NEXIS ion thruster.

By using numerical simulations and finite element analysis, this paper studies the plasma characteristics of LIPS-300 ion thruster's 20A emission current hollow cathode from the whole emitter region to plume region. Furthermore, the advantages and disvantages of the two methods are compared and evaluated by the hollow cathode operating performance testing. Finally, we evaluate the structure design of the 20A hollow cathode and give some suggestions for calculating the plasma parameters.

II. Initial conditions of the discharge region

The discharge process of hollow cathode is shown in Fig. 1. The emitter will produce electrons and form a thermal-electron current after heating to a certain temperature, a voltage is applied to the keeper of hollow cathode to generate an electric field between keeper and emitter region to accelerate the electrons which will then collide with the neutral xenon atom in emitter region. The high density plasma is then formed in emitter region and extracted to orifice region by the electric field between keeper and plasma sheath. Electrons in the plasma will continue to collide with neutral xenon atom in orifice region which causing the electrons growing rapidly by ionization process. Finally, the electrons are pulled into the plume region by the electric field between th keeper and the anode and become primary electrons in ion thruster's discharge chamber.

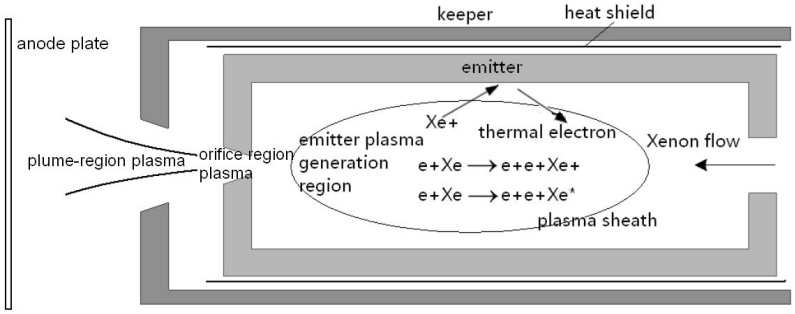

Fig.1 Discharge process of a hollow cathode

Figure 2 shows the whole discharge region of the 20A emission current hollow cathode according to the real structure. The length of the emitter is 10mm and its inner diameter is in the range of 2~2.5mm. The diameter and length of the cylindrical section of the orifice is 1mm and 2mm. The angle of cone section of the orifice is 45°. The distance from the keeper to the anode plate is 8mm and the internal surface area of the emitter is about 1.5cm^2. Before numerically calculating the plasma characteristics in the discharge region, the initial conditions has to be considered carefully including the electric field, xenon atom speed and neutral atom density.

The mass flow rate of 20A emission current hollow cathode is 0.2 mg/s and the exit pressure is about 450 Pa measured by a flowmeter. According to the former study results[5], the entrance pressure of the cathode tube and the exit pressure of orifice are 260.5 Pa and 76 Pa, respectively. As the gas in the supply tube is a viscous fluid, the simulation results of the pressure distribution, xenon velocity and neutral atom density in discharge region of hollow cathode by COMSOL are shown in Fig. 2(a), Fig. 2(b) and Fig. 2(c) with assumming the gas to be a steady flow. Before the cathode discharging, the potentials of the emitter and orifice plate are zero while the anode plate

potential is 25V. The distribution of electric field by ignoring the keeper potential is shown in Fig. 2(d).

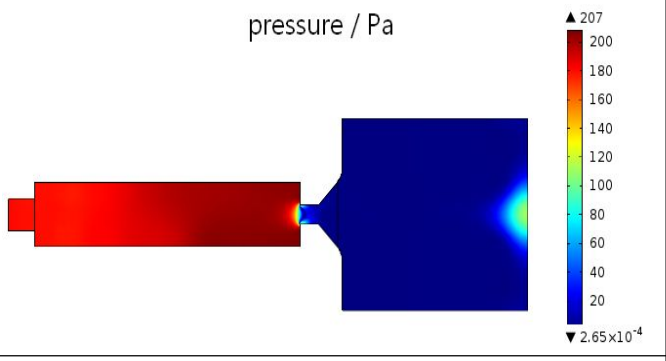

(a) pressure distribution of discharge region

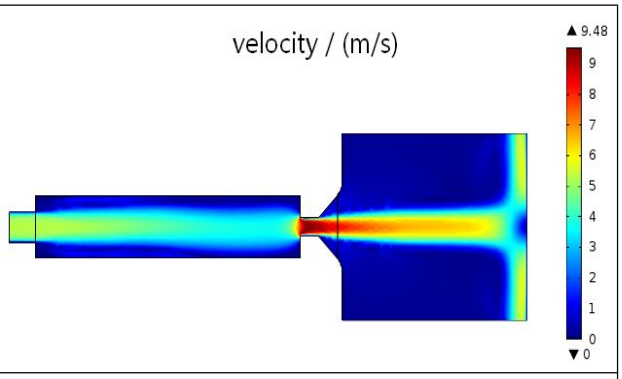

(b) xenon velocity in discharge region

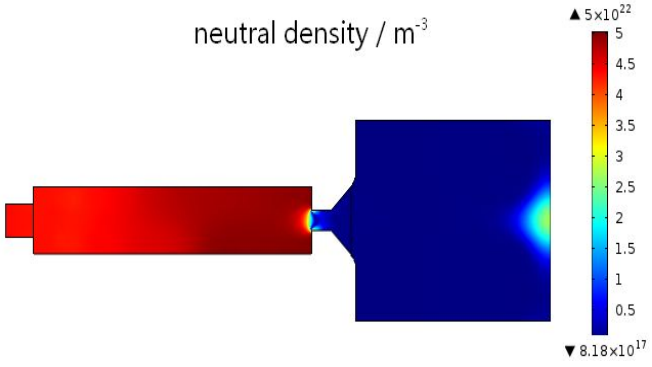

(c) neutral density distribution

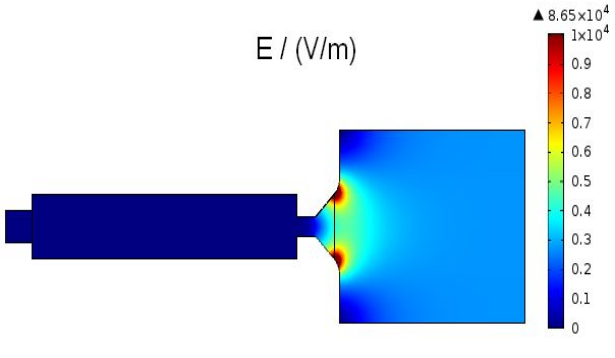

(d) electric field distribution

Fig.2 Initial conditions in the hollow cathode before discharging

III. Numerical calculation model

After obtaining the initial conditions in the discharge region, the plasma characteristics mainly including the electron temperature, plasma density, electron current density and ion current density are simulated by the fluid method. As the three discharge regions are discontinuous, different calculation model should be applied for each region. For simplicity, equations are solved in 0 dimension or one dimension in this paper and only the on-axis results are given due to the axisymmetric cathode.

a) Plasma simulation model in the emitter region

As the emitter region is the source of thermal electron emission and particle collision, plasma characteristics should be considered firstly. Electron temperature T_e is solved by the 0-D particle energy balance equation[6] which is given by

$$I_t\phi_S + RI_e^2 = I_iU^+ + 5T_eI_e/2 + (2T_e + \phi_S)I_re^{-\phi/T_e} \quad (1)$$

where I_t is the thermionic electron current (15A), ϕ is the cathode sheath voltage, R is the plasma resistance, which is expressed as $R = \eta l/\pi r_1^2$ (η is plasma resistivity, l is the emitter length, r_1 is inner diameter of emitter), I_e is the hollow cathode discharge current, I_i is the total ion current generated in the emitter region, U^+ is the ionization potential, I_r is the random electron flux at the plasma sheath edge (expressed in current). The expressions of I_i, I_r and I_e are given by Goebel[7] and Miller[8]. The plasma density, n_e, in discharge region is the same with the ion density when the discharging is steady which is given by

$$n_e = n_0e^{e\phi/kT_e} \quad (2)$$

where n_0 is the neutral xenon atom density. The electron current density J_e is solved by electron energy balance equation, which is given by:

$$-\nabla\cdot\left(-\frac{5}{2}\mathrm{J}_e\frac{kT_e}{e}-\kappa\frac{\nabla kT_e}{e}\right)+\eta J_e^2-\mathrm{J}_e\frac{\nabla n_e kT_e}{n_e e}-\dot{n}_e eU^+=0 \tag{3}$$

where κ is thermal conductivity of the plasma[9], k is Boltzmann constant, $\dot{n}_e$ is the generation rate of plasma which is given by plasma ambipolar diffusion equation as

$$\frac{\partial n_e}{\partial t}-D_p\nabla^2 n_e=0 \tag{4}$$

where D_p is ambipolar diffusion coefficient, which is dependent to the ion thermal velocity, ion mean collision frequency and CEX collision cross section (10^{-18} m^2).

The ion current density J_i is solved by ion energy balance equation as expressed by

$$-\nabla\cdot\left(-\frac{5}{2}\mathrm{J}_i\frac{kT_i}{e}-\kappa_n\frac{\nabla kT_i}{e}\right)+v_i\cdot\nabla(n_e kT_i)+n_e M\nu_{in}v_i^2+Q_T=0 \tag{5}$$

where κ_n is neutral xenon thermal conductivity, which is the same as ion temperature in the steady discharging state[10], v_i is average ion velocity, M is ion mass and Q_T is Joule heat generated by the ion current flow through the plasma.

Equations (1) and (2) are solved by replace the variables to functions of T_e whose default value is in the range of 0.1eV~5eV and the step-size is 0.1eV. The left and the right side of the equations are calculated separately and the electron temperature along the axis of the cathode is obtained by solving the intersection point of the two curves. Equations (3) to (5) are solved by one dimension model. The relation between the plasma density n_e and the emitter length is obtained by a three order polynomial fitting. By ignoring the average collision frequency between ion and atom, as well as ion and ion, the plasma generation rate $\dot{n}_e$, then electron current density J_e and ion current density J_i are obtained by fitting the plasma temperature T_e and the emitter length with only considering the electron-ion collision.

b) Plasma simulation model in the orifice region

The electron temperature T_e in the orifice region is solved by 0-dimension particle balance model [8] based on ambipolar diffusion theory, which is given by

$$\left(\frac{r_2}{\lambda_{01}}\right)^2 n_0\sigma_i(T_e)\sqrt{\frac{8kT_e}{\pi m}}-D_p=0 \tag{6}$$

where r_2 is the radius of the cathode orifice, m_e is electron mass, λ_{01} is the first zero value of the zero-order Bessel function, $\sigma_i(T_e)$ is the ionization collision cross-section in different Maxwellian electron temperature[11-12]. In order to obtain λ_{01}, Equations (4) is rewritten in cylindrical coordinates, and the plasma density n is solved by separating of variables of the radial distribution function $f(r)$ and the axial distribution function $g(z)$, which is given by

$$\frac{1}{f}\frac{\partial^2 f}{\partial^2 r}+\frac{1}{rf}\frac{\partial f}{\partial r}+C_1^2+\alpha^2=-\frac{1}{g}\frac{\partial^2 g}{\partial^2 z}+\alpha^2=0 \tag{7}$$

where C_1 and α are the equation coefficients, λ_{01} can be obtained by solving the Bessel function. T_e is obtained by substituting all the parameters into Eq.(6) and the plasma density n_e in the orifice region is solved by one dimension ion continuity equation as

$$\pi r_2^2\left(-\frac{\partial n_e}{\partial t}+\frac{\partial v_i n_0}{\partial z}\right)-2\pi r_2 v_{wall} n_e=0 \tag{8}$$

where $\partial n_e/\partial t$ is plasma generation rate in the orifice region, which has a close dependence to neutral density n_0, plasma density n_e and electron average velocity $\bar{v}_e$ and can be expressed as $\dot{n}=4\sigma_i(T_e)n_0 n\bar{v}_e$, where v_i is ion average velocity, v_{wall} is particle velocity closed to the radial edge of the orifice and can be written as terms of ion radial average drift velocity v_r [14] which is given by

$$v_r=\frac{2.4^2}{2r\sigma_{CEX}n_0 v_{scat}}\frac{e}{M}\left(T_i+T_e\right) \tag{9}$$

where σ_{CEX} is charge exchange collision cross-section, v_{scat} is the ion scattering velocity which is given by $v_{scat}=\sqrt{v_{th}^2+(v_i-v_0)^2+v_r^2}$ (v_0 is neutral atom velocity, which can be solved by Poiseuille flow in cylindrical tube[15]). The electron current density J_e in the orifice region can be obtained by one dimension electron continuity equation as

$$\pi r_2^2\left(e\frac{\partial n_e}{\partial t}+\frac{\partial J_e}{\partial z}\right)=0 \tag{10}$$

According to the definition of current, the orifice should be the electron flux cross section. From Eq.(10), the increased electron current from entrance to exit of the orifice region mainly comes from the ionization in the orifice region.

The ion current density is solved by steady-state ion energy equation and momentum equation. The relation between the ion current density and electron current density after ignoring the term of neutral atom's momentum[16] can be expressed as

$$J_i=\frac{m\nu_{en}}{M\nu_{in}(1+\nu_{ie}/\nu_{in})}J_e-\frac{\nabla(nkT_i+nkT_e)}{M\nu_{in}(1+\nu_{ie}/\nu_{in})} \tag{11}$$

where ν_{ie} is the collision frequency between electrons and ions, ν_{en} is the collision frequency between electrons and atoms[11-12].

The radial and axial neutral xenon density are fitted by second-degree polynomial fitting method respectively. There are 10 points in the radial direction with a step size of 0.2mm, and 10 points in the axial direction with a step size of 0.05mm. The radial and axial electron temperatures can be obtained by substituting the neutral xenon density , λ_{01} , and collision cross-section into Eq.(6). The plasma density can be obtained by substituting v_r, v_{wall}, $\dot{n}_e$, n_0 and the average of electron temperature into Eq.(8). The electron current density and the ion current density in the range of 0~2 mm of the orifice region can be obtained by solving Eq.(10) and Eq.(11) as one dimensional solution differential equation, respectively.

c) Plasma simulation model in the plume region

The plume region is the last ionization area in hollow cathode. As the neutral xenon diffusion process is the dominant position, the collision frequency is decreased significantly. Therefore, particle diffusion equation (shown in Eq.(4)) is adopted to obtain the plasma density in plume region. the electron current density J_e in the plume region could be describe by ion and electron momentum equation[18] as

$$J_e = \frac{1}{\eta}\left(E + \frac{\nabla n_e T_e}{n_e} \right) \tag{12}$$

According to Goebel's research results, for the plasma potential mutation in the orifice and plume region, the plasma potential changes about 7~8V of 25A emission current hollow cathode of NEXIS ion thruster and a double plasma sheath occurrs in the potential mutation area. The ion current density J_i and electron current density J_e passing through the double plasma sheath[19] can be calculated by

$$J_i = \frac{J_e}{k_v}\sqrt{\frac{m_e}{M}} \tag{13}$$

where k_v is the proportionality coefficient between the electron drift speed and the electron thermal speed.

IV. Comparation of numerical results and FEM results

In order to compare the difference of plasma characteristics obtained by different calculation methods, some simulations has been done by COMSOL to compare with the third section numerical results. The FEM calculation used in COMSOL is the drift-diffusion module which including the electron continuity equation, electron drift-diffusion equation, electron flux equation and energy equation. The electron drift-diffusion equation and energy equation are given by

$$\Gamma_e = -(\mu_e \cdot E) n_e - D_e \cdot \nabla n_e \tag{14}$$

$$\frac{\partial n_\varepsilon}{\partial t} + \nabla \Gamma_\varepsilon + E \cdot \Gamma_e = S_{en} - (u \cdot \nabla) n_\varepsilon \tag{15}$$

where E is the self-consisitent field, μ_e is electron migration coefficient, which is given by $\mu_e = e / m\nu(1+\Omega_e^2)$ (ν is the frequency of collisions between particles[17] and determined by the electron temperature). The term of electron Hall parameter correction Ω_e is ignored as there is no magnetic field. D_e is the electron diffusion coefficient which has Einstein's relation with μ_e. The electron generation rate R_e is mainly composed of excitation collision and ionization collision and can be expreesed as $n_0 n_e \langle \sigma\nu \rangle$, where the collision reaction coefficient $\langle \sigma\nu \rangle$ is given by Mikellides[20]. S_{en} is the energy loss of electron collision, n_ε is the electron energy density and Γ_ε is the electron energy density flux which are all have relations with μ_e, n_e and T_e.

The boundary condition of the model solution is set as follows: the anode plate is treated as the electron outlet which is given by $-n \cdot \Gamma_e = 0$. The emitter surface is set to be the thermal electron emission boundary, and other surface in the model of hollow cathode are set to be insulation boundary where the secondary emission is ignored. The initial value of the plasma density and the electron temperature is set to be 1×10^{20} m^{-3} and 3eV respectively and the solution time is set from 1×10^{-6} s to 0.01 s. The equations are solved by using the neutral density and electric field distribution calculated from Fig.2. The simulated plasma characteristic parameters are shown in Fig.3.

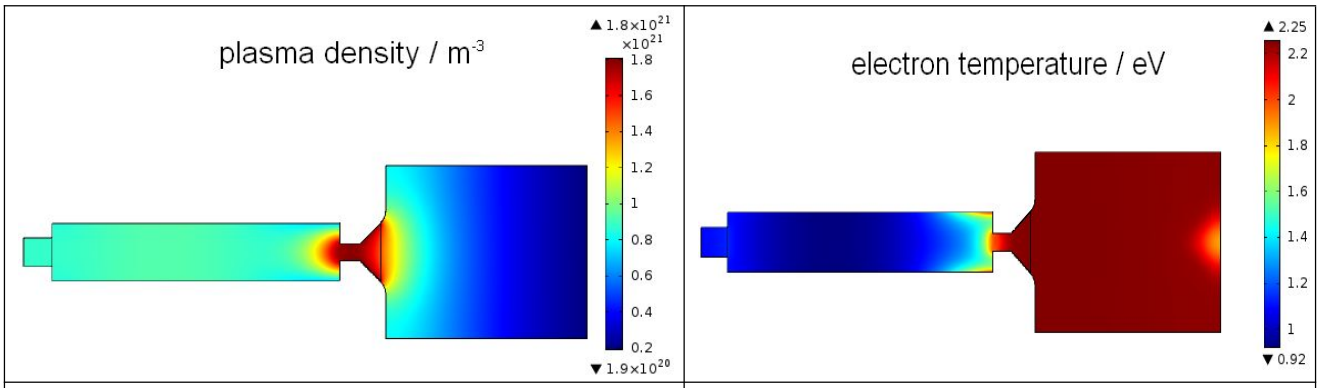

(a) plasma density in discharge region

(b) electron temperature

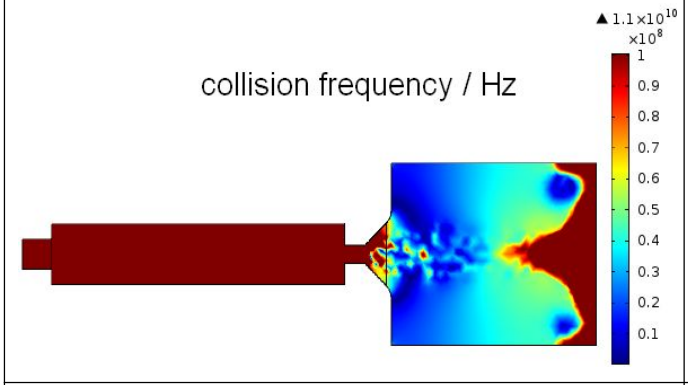

(c) collision frequency in discharge region

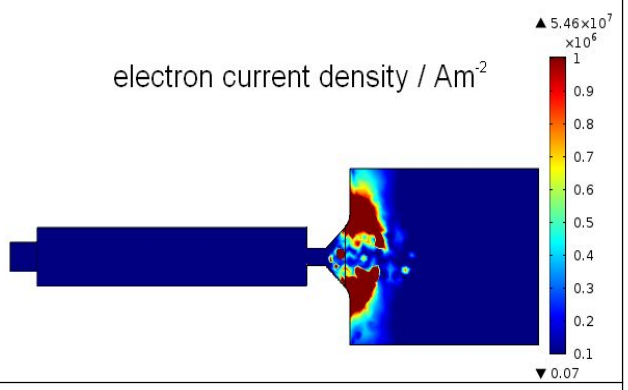

(d) electron current density

Fig.3 Plasma characteristics in the discharge region of the hollow cathode

Fig.4 shows comparison results of the plasma parameters in the discharge region of the hollow cathode for numerical method and FEM method. The discharge region is divided into three parts according to the actual size of the cathode. The plasma density, electron temperature and electron current density are shown in Fig.4(a)~Fig.4(c) respectively. In Fig.4(d), the ion current density calculated by numerical method is given while the FEM results is not.

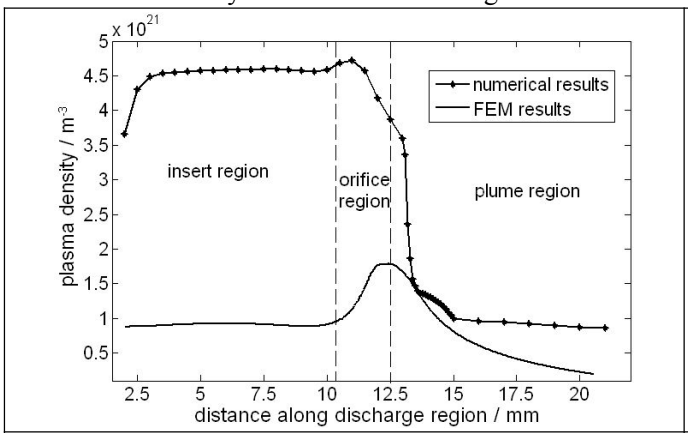

(a) plasma density

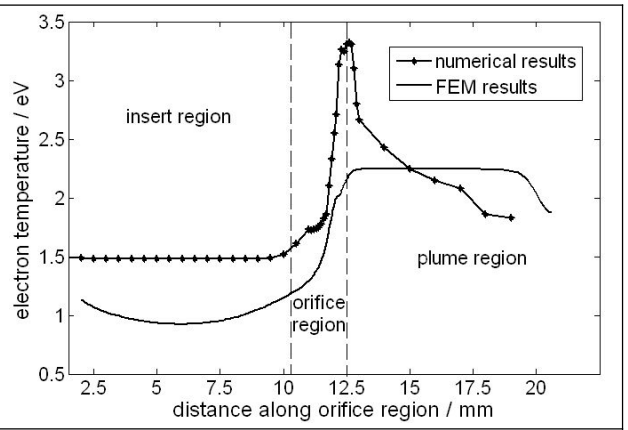

(b) electron temperature

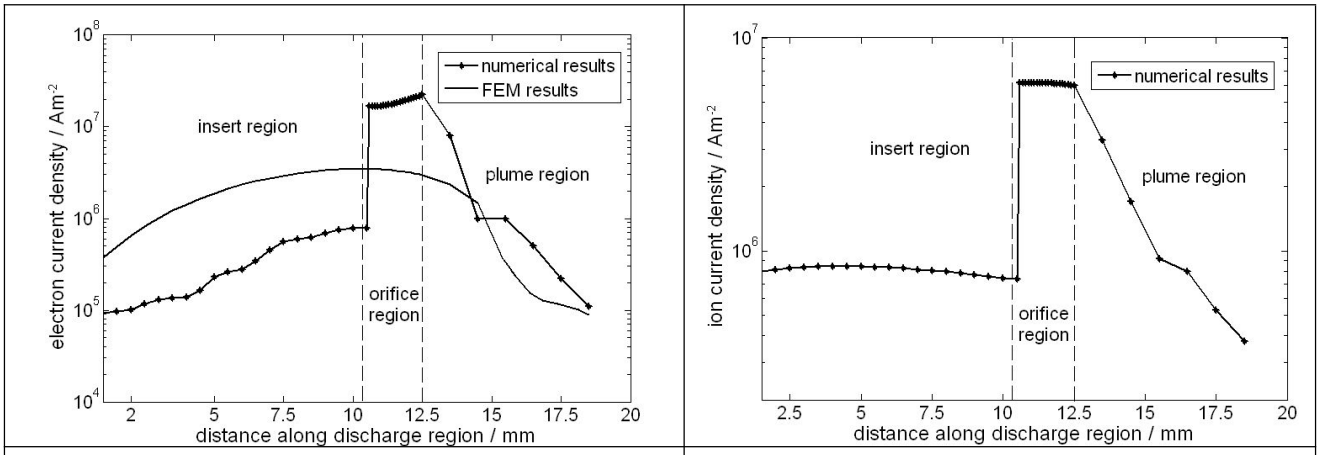

(c) electron current density (d) ion current density

Fig.4 The comparison of plasma characteristics of numerical and FEM results

Both the numerical calculation results and FEM results in Fig.4(a) show that the magnitude of the plasma density is about 10^{21} m^{-3} with an uniform distribution. The orifice region's plasma density is the highest in the whole discharge region of the cathode while the plasma density decreases exponentially along with the distance of the the orifice exit in the plume region. The reason of this phenomenon is that the neutral density distribution is more uniform in the emitter region and the Laval effect between two side ofthe orifice region which causing the neutral density to be highest in the internal orifice and the density drops rapidly along the exit direction. The decreasing of the neutral density n_0 causes the drop of ionization efficiency and the plasma generation rate according to the ion continuity equation which makes a plasma density distribution as shown in Fig. 4(a).

As shown in Fig.4(b), the electron temperature distribution obtained by two methodes is more uniform in the emitter region and significantly improved in the orifice region. The electron temperature increased about 1~2eV, in other words, the electron (include primary and secondary) energy is increased persistently in the discharge region from the generation to the extraction. The reason which caused this phenomenon is the increasing of the ambipolar diffusion coefficient D_p due to the decreasing of the interaction between particles which causes the electron temperature increasing significantly in the orifice region. With the drifting of electrons and the decreasing of the plasma sheath potential and further tending to steady in the plume region, the electron temperature changes correspondingly.

The electron current density calculated by two method is shown in Fig.4(c). The numerical results shows that the electron current desity changes from 10^5A/m^2 to 10^5A/m^2 while no current density jumps in the FEM method results. The reason which causing the phenomenon is the discontinuity of 0-D and 1-D plasma model in the numerical method, while based on drift-diffusion equation, the FEM method has continuity. Although there are some inconsistency between these two methods' calculation results, the varying tendency of the current density (the highest electron current density in the orifice region and dropped in the plume region) is similar. Considering the radial cross-section of the orifice, about 7.85×10^{-7} m^2, the axial electron current in the inlet and outlet of the orifice region is about 7.2A and 11.6A, respectively. The additional electron current is about 36% of the total emission current (the current enter the discharge chamber of the ion thruster) of the hollow cathode. The reason why the electron current density increases significantly is the higher ionization intensity in the orifice region, which can enhance the current gain which is

entirely determined by ionization intensity to the electron current flowing into the orifice region. Considering the internal factors which influence the ionization intensity, one can think that the current gain is determined by neutral density, gas temperature, orifice diameter and other parameters together.

The ion current density calculated by numerical method is shown in Fig.4(d). The FEM result is not given as the electron drift-diffusion model is applied. As shown in this figure, the varying trendency of the ion current density and the electron current in the whole discharge region is similar, which the highest ion current density is about $5\times10^6 A/m^2$.

V. Experimental results

The plasma characteristics of the 20A hollow cathode can not be diagnosted experimently yet. However, the emission current (same as electron current in the orifice outlet) can be estimated by the ion thruster's performance testing. According to the current balance relation in discharge chamber of thruster[21], the emission current I_e equal to the discharge current I_d subtract beam current I_b and keeper current I_k. The emission current is in the range of 19A~20A evaluated from LIPS-300 ion thruster's beam current (in the range of 3.4A~3.7A) testing results during 240min as shown in Fig.5(a).

From the Fig.5(b), the emission current of hollow cathode is gradually increased and became stable in 180min. The increasing of the emission current in earlier 40min is caused by the hot-gap changed during grids warm-up process. The increasing of the emission current in the later is caused by the continuously dropping of the beam current I_b at the beginning of the experiment. According to the Fig.5(b)'s results, the emission current is in the range of 11A~12A when thruster operating stably which is in well agreement with numerical results of increasing of the emission current in the orifice outlet in Fig.4(c). The simulation results show that the structure design of emitter and the orifice of hollow cathode well meet the thruster requirement and the numerical calculation results are in agreement with the experimental results.

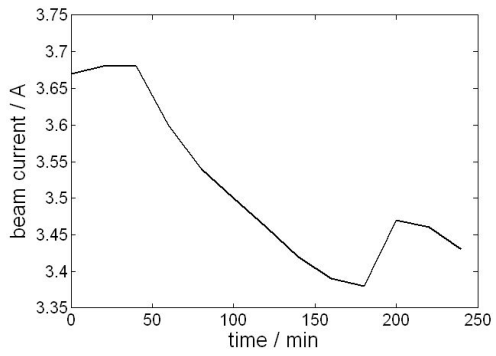

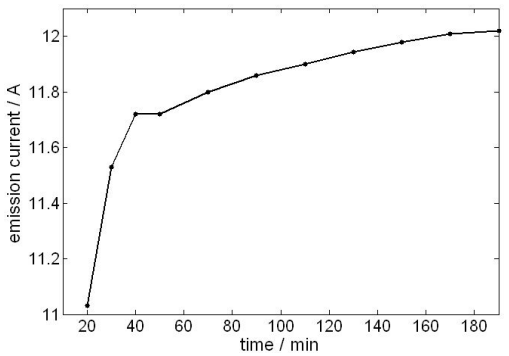

beam current / A | emission current / A

Fig.5 Beam current and emission current test results of 30cm ion thruster

VI. Conclusions

This paper describes the plasma characteristic in the entire discharge region of the 20A hollow cathode. The simulation results show that in the emitter region, the plasma is weakly ionized, quasi-neutral with relatively slow diffusion limited ion transport. The electron temperature is about 1.5eV in the emitter region and plasma density is in $10^{20}/m^3$ order. While in the orifice region, the electron temperature increased to the range of 2~4eV for the violent collisions between particles, and the current density is the highest in the hollow cathode which is in $10^{21}/m^3$ order, almost an

order greater than the emitter region. The plasma density decreases exponentially along with the distance of the orifice exit in the plume region where the electron temperature decreased rapidly to 2eV as the collision frequency decreasing with distance. The current structure design of hollow cathode is verified by the experimental results, which also proved the reliability of a type-A orifice (a small orifice with a large length-to-diameter ratio) adopted in hollow cathode of LIPS-300 ion thruster. With the results of two methods described in section 4, the FEM method does not show the significantly increasing of the electron current in the orifice region. The varying tendency of the plasma density and the electron temperature are in well agreement with numerical results which are also inconsisitent with the test results. Although the FEM results have few mistakes, it can still be used to estimate the discharge parameters in primary cathode design due to its simplicity.

Acknowledgement

Project supported by the Key Laboratory fund (Grant No. 6142207030103), and the National Natural Science Foundation of China (Grant Nos. 61601210)

References

[1]M.M. Sun，T.P. Zhang，L. Wang，X.M. Wu. Thermal Stress and Thermal Deformation Analysis of Grids Assembly for 30cm Diameter Ion Thruster[J]．*Journal of Propulsion Technology*，2016，37(7):1393-1400.

[2]D Goebel, K Jameson, I Katz, et al. Hollow cathode Theory and Modeling:I. Plasma Characterization with Miniature Fast-Scanning Probes[J]．*Journal of Applied Physics*，2005，98(10):113302.

[3]I Katz, J Anderson, J Polk, et al. A Model of Hollow Cathode Plasma Chemistry[R]. AIAA paper. 2002-4241.

[4]Malik A, Montarde, B Haines, et al. Spectroscopic Measurements of Xenon Plasma in a Hollow Cathode[J]．*Journal of Applied Physics*，2000，33(3):2307-2048.

[5]M.M. Sun，T.P. Zhang，X.M. Wu. Flow field simulation of 20 cm diameter ion thruster discharge chamber. *High Power Laser and Particle Beams*, 2015, 27(5): 054001

[6]D Goebel, I Katz. Fundamentals of Electric Propulsion:Ion and Hall Thrusters[M]. JPL Space Science and Technology Series, 2008:259-260.

[7]J Miller, S Pullins, et al. Xenon Charge Exchange Cross Sections for Electrostatic Thruster Models[J]．*Journal of Applied Physics*，2012，91(3):984-991.

[8] K Jameson, D Goebel, R Watkins. Hollow Cathode and Keeper-Region Plasma Measurements[R]. AIAA paper. 2005-3667.

[9]R Wirz, I Katz. Plasma Processes of DC Ion Thruster Discharge Chambers[R]//AIAA. 2005. 3690-3695.

[10]I Mikelides, I Katz, D Goebel, et al. Theoretical Model of a Hollow Cathode Plasma for the Assessment of Insert and Keeper Lifetimes[R]. AIAA Paper 2005-4234.

[11]Bond, Latham. Ion Thruster Extraction Grid Design and Erosion Modeling using Computer Simulation[R]. AIAA paper. 1995-2923.

[12]Rapp D, Francis. Charge Exchange Between Gaseous Ions and Atoms[J]. *Journal of Chemical Physics*. 1962,37(11):2631~2645

[13]J Polk, A Grubisic, N Taheri, et al. Emitter Temperature Distributions in the NSTAR Discharge Hollow Cathode[R]. AIAA Paper 2005-4398.

[14]I Mikelides, I Katz, D Goebel, et al. Plasma Processes Inside Orificed Hollow Cathode[J]. *Physics of plasmas*，2006, 13(5):063504.

[15]I Katz, J Anderson, J Polk, et al.One Dimensional Hollow Cathode Model[J]. *Journal of Propulsion and Power*, 2003, **19**(4):595–600.

[16]I Mikelides, I Katz, D Goebel, et al. Hollow cathode Theory and Modeling : II. A Two-Dimensional Model of the Emitter Region[J]．*Journal of Applied Physics*，2005，98(10):113303.

[17]D Book. NRL Plasma Formulary[M]. Washington D C: Naval Research Laboratory, 1987:402-410.

[18]I Katz, I Mikellides, D Goebel. Model of the Plasma Potential Distribution in the Plume of a Hollow Cathode[R]. AIAA Paper 2004-4108.

[19]I Langmuir. The Interaction of Electron and Positive Ion Space Charges in Cathode Sheaths[J]．*Physical Review*，1929，33(6):954-989.

[20]I Mikelides, I Katz, M Mandell. A 1-D Model of the Hall-Effect Thruster with an Exhaust Region[R]. AIAA Paper 2001-3505.

[21]J Matossian, J Beattie. Model for Computing Volume Averaged Plasma Properties in Electron-Bombardment Ion Thruster[J]. *Journal of Propulsion and Power*，1989, 5(1):188-196.

*corresponding author

E-mail address: smmhappy@163.com